Carbohydrate Polymers 79 (2010) 1140–1149

Contents lists available at ScienceDirect

Carbohydrate Polymers

journal homepage: www.elsevier.com/locate/carbpol

Characterization of modified wheat straw, kinetic and equilibrium study about copper ion and methylene blue adsorption in batch mode

Runping Han *, Lijun Zhang, Chen Song, Manman Zhang, Huimin Zhu, LiJuan Zhang

Department of Chemistry, Zhengzhou University, No. 100 of Kexue Road, Zhengzhou 450001, PR China

ARTICLE INFO

Article history:
Received 15 September 2009
Received in revised form 19 October 2009
Accepted 22 October 2009
Available online 25 October 2009

Keywords:
TG analysis
FTIR analysis
Modified wheat straw
Copper ion
Methylene blue
Adsorption

ABSTRACT

The citric acid modified wheat straw (MWS) was characterized and the adsorption properties of copper ion and methylene blue (MB) onto MWS were investigated in single adsorbate system by batch techniques. The mass loss during thermo-gravimetric analysis can be divided into steps related to moisture, cellulose and lignin. There were carbonyl group, hydroxyl group, etc. on surface of adsorbent from FTIR. Kinetic studies indicated that Cu^{2+} and MB adsorption followed the pseudo-second-order model. The adsorption may be controlled by external mass transfer followed by intra-particle diffusion mass transfer. The adsorption equilibrium data were fitted well by both the Freundlich and Langmuir models. The maximal equilibrium quantity of Cu^{2+} and MB from Langmuir model on MWS was 39.17 and 396.9 mg g^{-1} at 293 K, respectively. The thermodynamics parameters of adsorption systems indicated spontaneous and endothermic process.

1. Introduction

There are many billion kilograms of agricultural waste products in China. These materials are considered a significant waste disposal problem. They are often used as foodstuff, energy fuel, or compost, etc. But many are treated as waste. So it is promising to develop the other ways in order to utilize these by-products. Agricultural waste materials are economic and eco-friendly due to their unique chemical composition, availability in abundance, renewable, low in cost and more efficient, and are seem to be viable option for heavy metal and dye remediation (Crini, 2006; Gupta & Ali, 2008; Gupta & Suhas, 2009; Khan, Li, & Huang, 2008; Sud, Mahajan, & Kaur, 2008; Wan Ngah & Hanafiah, 2008). Some of these by-products such as rice husk, wheat straw, cereal chaff, wheat husk, peanut hull, soybean hulls, hazelnut shells, sugar beet pulp, e-oiled soya, carbon from wood and fallen leaf, etc. have been used to remove metal ions or dyes from solution (Ahluwalia & Goyal, 2007; Cimino, Passerini, & Toscano, 2000; Dang, Doan, Dang-Vuc, & Lohi, 2009; Gupta, Jain, & Varshney, 2007; Gupta, Mittal, Krishnan, & Mittal, 2006; Han, Ding, et al., 2008; Han, Han, et al., 2008; Han, Wang, et al., 2006, 2009; Han, Zhang, Zou, Shi, & Liu, 2005; Han, Zhang, et al., 2006; Han et al., 2007; Krishnani, Meng, Christodoulatos, & Boddu, 2008; Sud et al., 2008; Teixeira Tarley & Zezzi Arruda, 2004; Tsang et al., 2007; Wu et al., 2009). There are several advantages over commercial resins and activated carbon in that they are less expensive, biodegradable and come from renewable resource.

However, the application of untreated plant wastes as adsorbents can also bring several problems such as lower adsorption capacity, higher chemical oxygen demand (COD) and biological chemical demand (BOD) as well as total organic carbon (TOC) due to release of soluble organic compounds contained in the plant materials (Wan Ngah & Hanafiah, 2008). Therefore, plant wastes need to be modified or treated before being applied for the decontamination of heavy metals and dyes. Furthermore, modification of agricultural by-products can be carried out to achieve adequate structural durability, enhance their natural ion exchange capability and add value to the by-product (O'Connell, Birkinshaw, & O'Dwyer, 2008; Vaughan, Seo, & Marshall, 2001).

Pretreatment methods using different kinds of modifying agents such as base solutions (sodium hydroxide) mineral and organic acid solutions (hydrochloric acid, phosphoric acid, tartaric acid, citric acid, thioglycollic acid), organic compounds (ethylenediamine, formaldehyde), etc. for the purpose of removing soluble organic compounds, eliminating color of the aqueous solutions and increasing efficiency of metal and dye adsorption have been performed by many researchers (Gong, Sun, et al., 2008; Gong, Zhong, et al., 2008; Gong, Zhu, et al., 2008; Gurgel, Freitas, & Gil, 2008; Marshall, Wartelle, Boler, Johns, & Toles, 1999; Ong, Lee, & Zainal, 2007; Šæiban, Klašnja, & Škrbiæ, 2008; Vaughan et al., 2001; Wong, Lee, Low, & Haron, 2003). But these studies only discuss the adsorptive behavior of metal ions or dyes.

* Corresponding author. Tel.: +86 371 67781757; fax: +86 371 67781556.
E-mail address: rphan67@zzu.edu.cn (R. Han).

0144-8617/$ - see front matter © 2009 Elsevier Ltd. All rights reserved.
doi:10.1016/j.carbpol.2009.10.054

Wheat straw is abundant and inexpensive in north region of China. It is often used as a waste or feedstuff. Wheat straw has been used as adsorbent to remove heavy metal ions (Dang et al., 2009; Doan, Lohi, Dang, & Dang-Vu, 2008) and dyes from solution (Robinson, Chandran, & Nigam, 2002). Thermo-chemical esterifying citric acid on wheat straw can enhance wheat straw ability of cationic dye adsorption. But there is few study on the research which simultaneously discuss the behavior of metal and dye adsorption onto agricultural by-product, except other materials used as adsorbents (Aksu & Isoglu, 2007; Wang & Ariyanto, 2007; Wu et al., 2009).

The objective of this study was to modify wheat straw with citric acid to enhance the adsorption capacity of the by-product for selected copper ions and methylene blue (MB). The characterization of natural wheat straw (NWS) and modified wheat straw (MWS) was analyzed by FTIR, TGA–DSC (thermo-gravimetric analysis and differential scanning calorimetry) and scanning electron micrograph (SEM) method.

2. Materials and methods

2.1. Preparation of MWS

The wheat straw used in the present investigation was obtained from local countryside. The collected materials were washed with distilled water for several times to remove all the dirt particles. The washed material was dried in an oven at 373 K for a period of 24 h. Then dried straw segment was milled and sieved to retain the 20–40 mesh fractions for chemical modification.

MWS was prepared according to the modified method (Vaughan et al., 2001). Ground wheat straw was mixed with 0.6 mol l^{-1} citric acid (CA) at the ratio of 1:12 (straw/acid, w/v) and stirred for 30 min at 20 °C. The acid straw slurries were placed in a stainless steel tray and dried at 50 °C in a forced air oven for 24 h. Then the thermo-chemical esterification between acid and straw was proceeded by raising the oven temperature to 120 °C for 90 min. After cooling, the esterified wheat straw was washed with distilled water until the liquid did not turn turbidity when 0.1 mol l^{-1} lead (II) nitrate was dropped in. After filtration, MWS was suspended in 0.1 mol l^{-1} NaOH solution at suitable ratio and stirred for 60 min, followed by washing thoroughly with distilled water to remove residual alkali, next dried at 50 °C for 24 h and preserved in a desiccator for use.

The chemical modification of wheat straw can be schematically expressed by equation (Gong, Zhong, et al., 2008):

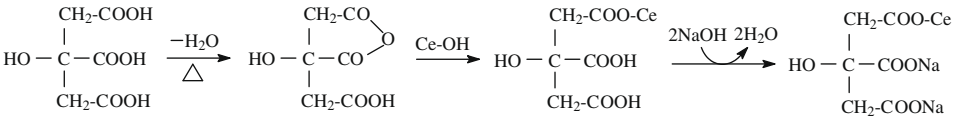

Note: Ce-OH—Natural wheat straw

2.2. Preparation of MB and copper ion solution

The MB and Cu^{2+} stock solutions were prepared by dissolving accurately weighted dyes and $CuCl_2$ in distilled water to the concentration of 1000 mg l^{-1} and 500 mg l^{-1}, respectively. The experimental solutions were obtained by diluting the dye or Cu^{2+} stock solutions in accurate proportions to different initial concentrations. As experiment result proved that the optional value of solution pH for Cu^{2+} and MB is 5 and 4–10, respectively, the initial pH of the working solution was adjusted by addition of 1 mol l^{-1} HCl or NaOH solution to near 5.

2.3. Experimental methods and measurements

The adsorption tests were performed by batch technique in single system at 293, 303, 313 K, respectively. For kinetic and isothermal studies, a series of 125 ml flask were used and each flask was filled with wheat straw at mass loadings 2 g l^{-1} for Cu^{2+} solution and 1 g l^{-1} for MB solution at different initial concentrations (10 ml), respectively. The conical flasks were then agitated in an orbital shaker at 100 rpm and liquid samples were taken out at a given time interval for Cu^{2+} or MB analyses after centrifugation.

Cu^{2+} concentration was measured using atomic absorption spectrometry at 234.8 nm (AAanalyst300, Perkin-Elmer). MB concentration is determined using a UV spectrophotometer (Shimadzu Brand UV-3000) by monitoring the absorbance changes at a wavelength of maximum absorbance (668 nm).

The data obtained in batch mode studies were used to calculate the equilibrium metal adsorptive quantity. It was calculated for each sample of Cu^{2+} or MB by using the following expression:

$$q_e = \frac{V(c_0 - c_e)}{1000m} \quad (1)$$

where q_e is the equilibrium uptake value (the amount of Cu^{2+} or MB adsorbed onto per unit mass of NWS) in mg g^{-1}, V is the sample volume in ml, c_0 is the initial Cu^{2+} or MB concentration in mg l^{-1}, c_e is the equilibrium adsorbent concentration in mg l^{-1}, and m is the dry weight of MWS in g.

2.4. Wheat straw characterization

The thermal behavior of NWS was obtained by using a thermo-gravimetric analyzer (STA 409 PC, German). About 10 mg of NWS were heated up to 600 °C in oxidant atmosphere at 10 °C min^{-1} temperature rate.

Photomicrography of the exterior surface of NWS and MWS was obtained by SEM (JEOL 6335F-SEM, Japan).

The functional groups present in the wheat straw were characterized by a Fourier transform infrared spectrometer (PE-1710, USA), using potassium bromide discs to prepare the NWS and MWS samples. The spectral range varied from 4000 to 400 cm^{-1}.

3. Results and discussion

3.1. Characterization of NWS and MWS

3.1.1. The curve of TG about NWS

Like all vegetable biomass, NWS are composed of cellulose, hemi-cellulose and lignin. Fig. 1 was shown the curve of TG and DSC about NWS.

The overall mass loss during thermo-gravimetric analyses can be divided into steps related to moisture, hemi-cellulose, cellulose

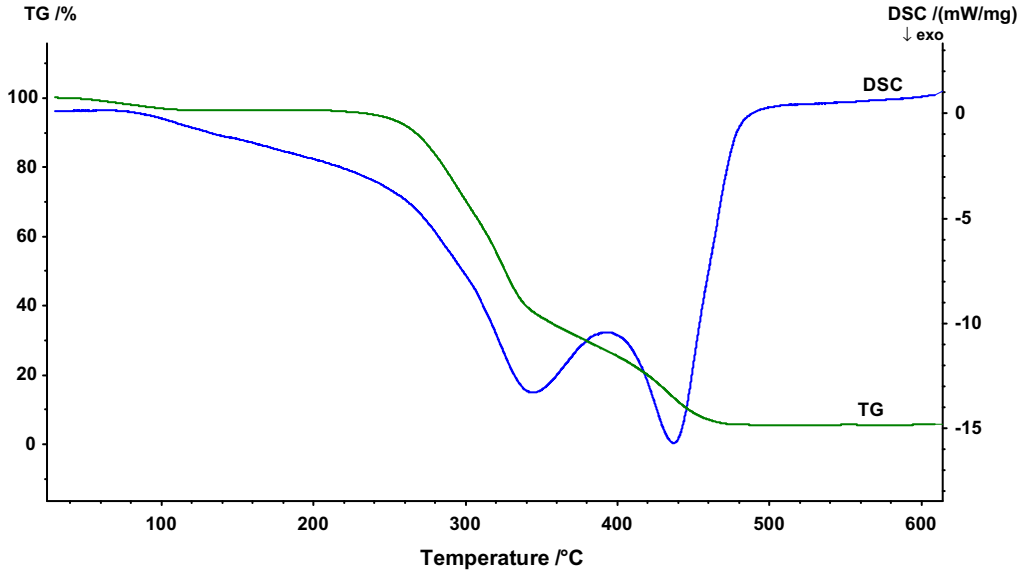

Fig. 1. Curves of thermo-gravimetric analysis (TGA) and differential scanning calorimetry (DSC) of native wheat straw.

and lignin (Fig. 1). Thus, as one can see, a mass loss of 3.65% by heating the wheat straw up to 140 °C was verified due to the elimination of moisture retained in this material. From 140 to 230 °C, mass loss was insignificant. Afterwards, the second step of pyrolysis was obtained when the temperature was varied from 230 to 380 °C. In this step, a higher mass loss (66.37%) was observed. The behavior of the pyrolysis curve at this temperature indicates hemi-cellulose and cellulose decomposition, as well as loss of the remaining adsorbed water. Lignin decomposition occurs in the 380–500 °C range (mass lose 24.45%), thus indicating that this structure presents higher stability than hemi-cellulose and cellulose. Finally, no mass loss was detected when the temperature was increased to 600 °C. This result indicates the presence of oxides (mainly those of aluminium and silicon), which are stable at higher temperatures.

From the DSC curve in Fig. 1, the max peaks at 325 °C and 430 °C were observed by exothermic decomposed reaction from cellulose and lignin, respectively.

3.1.2. SEM of NWS and MWS

Scanning electron micrographs of NWS and MWS were shown in Fig. 2.

The morphology of this material can facilitate the adsorption of metals and dyes, due to the irregular surface of the straw, thus makes possible the adsorption of adsorbate in different parts of this material. Further more, the surface of MWS is rougher than that of NWS. So, based on the morphology, it can be concluded that this material presents an adequate morphological profile to retain metal and dye ions (Teixeira Tarley & Zezzi Arruda, 2004).

3.1.3. FTIR of NWS and MWS

The FTIR technique is an important tool to identify some characteristic functional groups, which are capable of adsorbing metal ions and dye ions. Fig. 3 was shown the FTIR of NWS and MWS.

As shown in Fig. 3, the spectra displayed a number of absorption peaks, indicating the complex nature of the material. The broad absorption peaks around 3405 cm^{-1} were indicative of the existence of bonded hydroxyl groups on the surface of wheat straw. This band was due to vibration of the silanol group, hydroxyl group linked in cellulose and lignin, and adsorbed water on the straw surface. The peaks observed at 2917 and 1376 cm^{-1} were assigned to the stretch vibration and bending vibration of C–H bond in methyl group, respectively. The peaks located at 1736 and 1640 cm^{-1} were characteristics of carbonyl group stretching from aldehydes and ketones (Teixeira Tarley & Zezzi Arruda, 2004). These groups can be conjugated or non-conjugated to aromatic rings (1640 and 1730 cm^{-1}, respectively). The peak near 1425 cm^{-1} was also attributed to stretch vibration of C–O from carboxyl group. The peaks associated with the stretch vibration in aromatic rings were verified at 1603 and 1511 cm^{-1} while deformations related to C–H and C–O bonds were observed from 1085 to 1040 cm^{-1}. The strong C–O band at 1051 cm^{-1} also confirms the lignin structure of the wheat straw. The peak at 1248 cm^{-1} may be from the stretch vibration of C–O in phenols.

From Fig. 3, it was shown that modification brought increase of stretch vibration adsorption band of carboxyl group (at 1738 cm^{-1}) and C–O group (at 1592 cm^{-1}). The shift of some peaks changed after modification. The results showed that MWS had more carboxyl groups than NWS. The intensity is a function of the change in electric dipole moment and also the total number of such bonds in the sample. The band of C–O group is more intense than that of C=O group, possibly because of more C–O groups present in the adsorbent (Krishnani et al., 2008).

It was well indicated from FTIR spectrum of NWS and MWS that carboxyl and hydroxyl groups were present in abundance. These groups may function as proton donors, hence deprotonated hydroxyl and carboxyl groups may be involved in coordination with metal ions and action with positive dye ions.

From the characterization of MWS, the rough surface and functional groups made MWS's beneficial to adsorb metal and dye cation ion from solution.

3.2. Adsorption kinetic study

Fig. 4 illustrated the effect of contact time on adsorption of Cu^{2+} and MB on MWS at different temperature.

From Fig. 4, it was found that the adsorptive quantity of both Cu^{2+} and MB on MWS increased with the contact time increasing. A two-stage kinetic behavior was evident: an initial rapid stage where adsorption was fast and contributed significant to

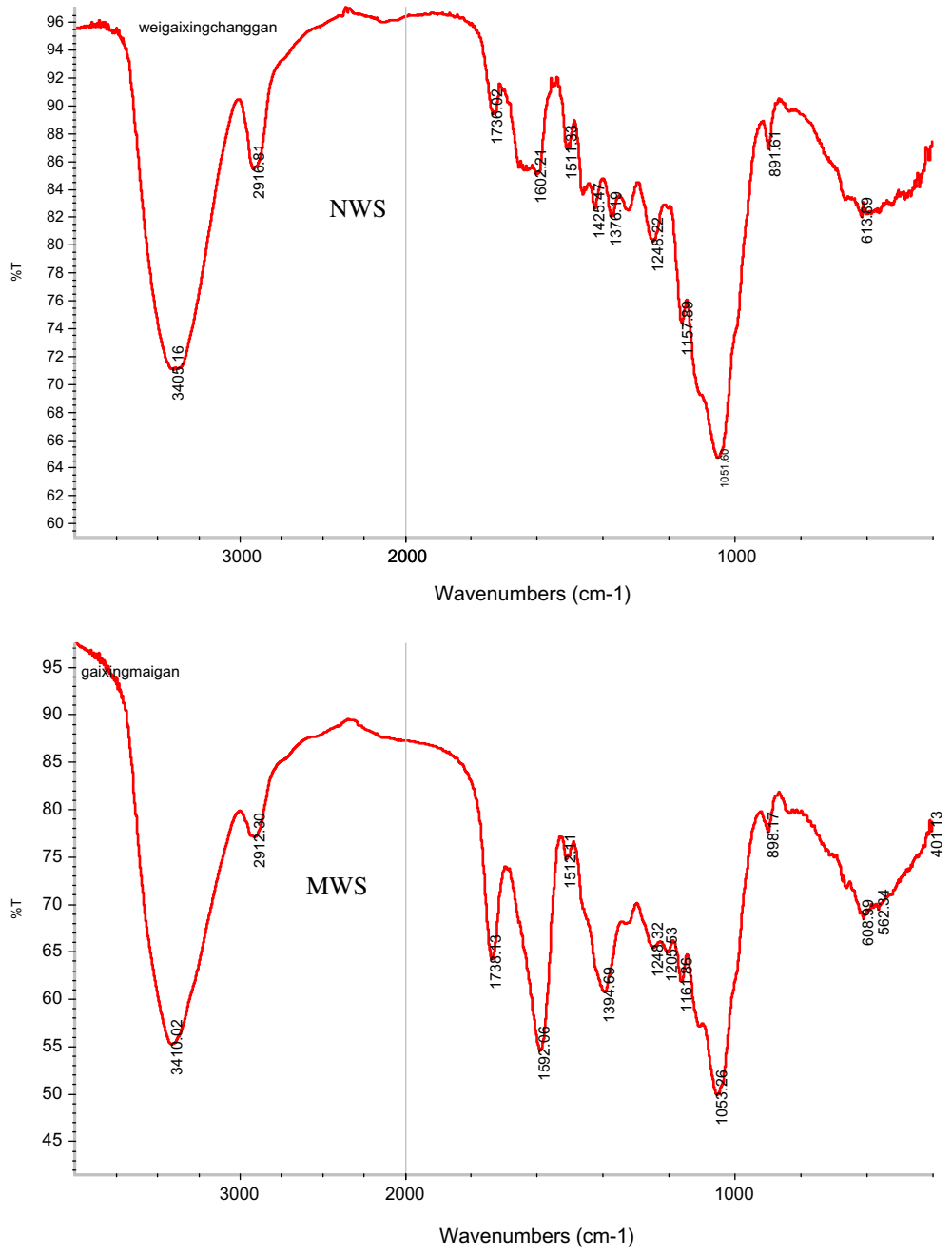

Fig. 2. Fourier transform infrared spectra of natural wheat straw (NWS) and modified wheat straw (MWS).

equilibrium uptake and a slower second stage whose contribution to the total MB adsorption was relatively small.

It was also seen from Fig. 4 that higher temperature was advantage of the increase in adsorption quantity. This indicated that the adsorption of Cu^{2+} and MB ions onto MWS was endothermic in nature.

Adsorption kinetics models are used to explain the adsorption mechanism and adsorption characteristics. Three simple kinetic models are used, which are pseudo-first-order, pseudo-second-order, Elovich equation. The pseudo-first-order equation is expressed as (Ho, Ng, & McKay, 2000):

$$q_t = q_e(1 - e^{-k_1 t}) \quad (2)$$

where q_e and q_t are the amount of solute adsorbed (mg g^{-1}) at equilibrium and time t (min), respectively, and k_1 is the rate constant of the pseudo-first-order adsorption (min^{-1}).

The pseudo-second-order equation is given by the following equation as (Ho & McKay, 1999; Ho et al., 2000):

$$q_t = \frac{k_2 q_e^2 t}{1 + k_2 q_e t} \quad (3)$$

where k_2 is the rate constant of the pseudo-second-order adsorption (mg g^{-1} min^{-1}).

The Elovich equation is expressed as (Cheung, Porter, & Mckay, 2000):

$$q_t = A + B \ln t \quad (4)$$

where A and B are the Elovich constant.

As different forms of the equation affected R^2 values more significantly during the linear analysis, the nonlinear analysis might be a method of avoiding such errors (Han, Zhang, et al., 2009).

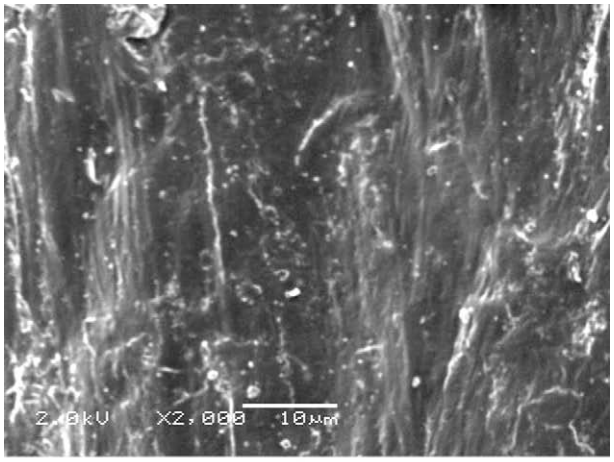

Fig. 3. SEM of native wheat straw (NWS) and modified wheat straw (MWS).

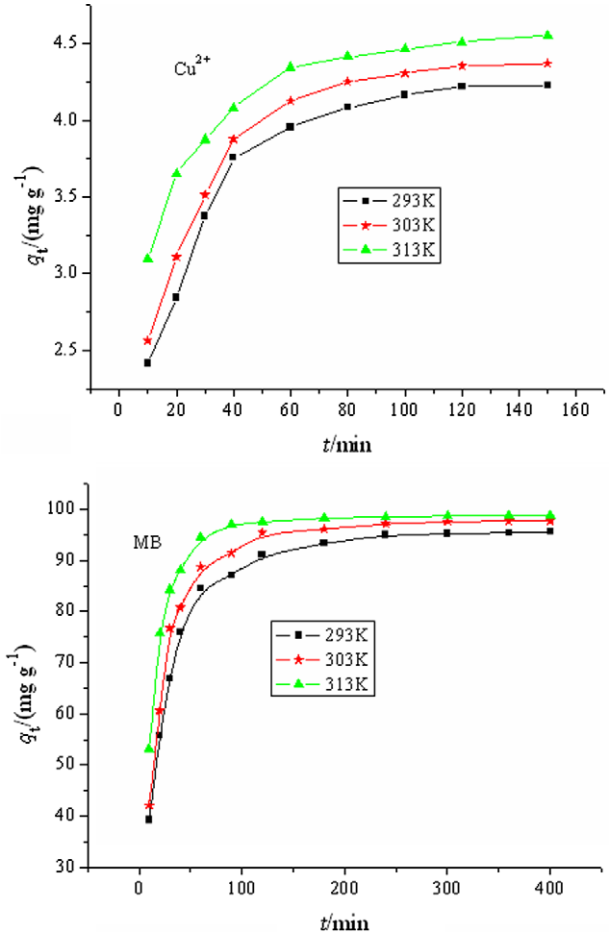

Fig. 4. Effect of contact time on adsorption of Cu^{2+} (c_0 = 10 mg l^{-1}) and MB (c_0 = 100 mg l^{-1}) by MWS.

The nonlinear regressive method of least sum squares of difference between calculated data and experimental data was used to determine the kinetic parameters, respectively. The results were listed in Tables 1 (for Cu^{2+}) and 2 (for MB), respectively.

From Table 1, the values of R^2 (bigger than 0.91) and x^2 (less than 0.0433) are only slightly difference about pseudo-first-order equation, pseudo-second-order equation and Elovich equation, respectively. The calculated values of q_e obtained from pseudo-first-order model and pseudo-second-order model agreed more perfectly with the experimental $q_{e(exp)}$ values of Cu^{2+} adsorption at three different temperatures, respectively. So it is concluded that three models can predict the kinetic process in experimental condition. Moreover, the best was pseudo-second-order model while the worst was the pseudo-first-order model.

But for MB adsorption, the best kinetic model was pseudo-second-order model while the worst was the Elovich equation according to values of R^2 and x^2 listed in Table 2. So the pseudo-second-order model can be used to predict the kinetic process for Cu^{2+} and MB adsorption.

The results showed that the process of Cu^{2+} and MB adsorption on MWS was chemical behavior (Ho & McKay, 1999). From FTIR of MWS, there was negative charge of carboxyl group ($-COO^-$) on the surface of MWS, but Cu^{2+} and MB existed in solution were positive. So it was referred that the main mechanism of the Cu^{2+} and MB adsorption behavior by MWS may be ion exchange.

Table 1
Kinetic parameters of Cu^{2+} adsorption onto MWS.

T/K	293	303	313
Pseudo-first-order equation			
k_1/(min^{-1})	0.0671 ± 0.0068	0.0725 ± 0.0072	0.104 ± 0.001
$q_{e(theo-1)}$/(mg g^{-1})	4.11 ± 0.09	4.24 ± 0.09	4.36 ± 0.08
$q_{e(exp)}$/(m g^{-1})	4.30	4.40	4.60
R^2	0.919	0.916	0.842
x^2 [a]	0.0397	0.0394	0.0433
Pseudo-second-order equation			
k_2/(g mg^{-1} min^{-1})	0.0220 ± 0.0022	0.0238 ± 0.0018	0.0387 ± 0.0022
$q_{e(theo)}$/(mg g^{-1})	4.56 ± 0.08	4.68 ± 0.05	4.70 ± 0.03
R^2	0.978	0.987	0.990
x^2	0.0109	0.00592	0.00272
Elovich equation			
A	0.882 ± 0.262	1.11 ± 0.24	2.02 ± 0.17
B	0.712 ± 0.065	0.695 ± 0.061	0.534 ± 0.043
R^2	0.944	0.950	0.957
x^2	0.0276	0.0236	0.0119
Intra-particle diffusion model			
K_{t1}/(mg g^{-1} $min^{-1/2}$)	0.430 ± 0.31	0.414 ± 0.003	0.309 ± 0.037
C_1/(mg g^{-1})	1.01 ± 0.15	1.25 ± 0.02	2.19 ± 0.19
R^2	0.989	0.999	0.971
x^2	0.00534	0.00006	0.0078
K_{t2}/(mg g^{-1} $min^{-1/2}$)	0.0613 ± 0.0125	0.0537 ± 0.0106	0.0459 ± 0.0029
C_2/(mg g^{-1})	3.52 ± 0.13	3.74 ± 0.11	3.99 ± 0.03
R^2	0.889	0.895	0.987
x^2	0.0019	0.0014	0.00011

[a] $x^2 = \sum(q_t - q_c)^2$, q_t and q_c are the experimental value and calculated value according the model, respectively.

Table 2
Kinetic parameters of MB adsorption onto MWS.

T/K	293	303	313
Pseudo-first-order equation			
k_1/(min^{-1})	0.0446 ± 0.0024	0.0513 ± 0.0022	0.0729 ± 0.0029
$q_{e(theo-1)}$/(mg g^{-1})	93.21 ± 1.12	95.87 ± 0.87	97.49 ± 0.68
$q_{e(exp)}$/(m g^{-1})	96.0	98.0	99.0
R^2	0.976	0.984	0.982
x^2	8.72	5.51	3.83
Pseudo-second-order equation			
k_2/(g mg^{-1} min^{-1})	0.00067 ± 0.00004	0.00079 ± 0.00007	0.00127 ± 0.00012
$q_{e(theo)}$/(mg g^{-1})	100.81 ± 0.92	102.94 ± 1.30	102.89 ± 1.17
R^2	0.991	0.979	0.968
x^2	3.25	7.07	6.77
Elovich equation			
A	17.04 ± 7.38	25.21 ± 8.60	45.84 ± 8.28
B	14.26 ± 1.59	13.31 ± 1.85	9.87 ± 1.78
R^2	0.890	0.838	0.754
x^2	40.93	55.64	51.52
Intra-particle diffusion model			
K_{t1}/(mg g^{-1} min$^{-1/2}$)	11.54 ± 0.35	12.78 ± 1.51	11.17 ± 2.15
C_1/(mg g^{-1})	3.42 ± 1.72	2.97 ± 7.55	21.08 ± 10.75
R^2	0.998	0.973	0.931
x^2	0.664	12.67	25.69
K_{t2}/(mg g^{-1} min$^{-1/2}$)	1.60 ± 0.24	2.06 ± 0.30	0.941 ± 0.31
C_2/(mg g^{-1})	72.32 ± 2.54	72.45 ± 2.89	87.50 ± 2.92
R^2	0.957	0.971	0.903
x^2	0.995	0.479	0.487
K_{t3}/(mg g^{-1} min$^{-1/2}$)	0.140 ± 0.014	0.243 ± 0.063	0.0789 ± 0.016
C_3/(mg g^{-1})	92.79 ± 0.24	93.09 ± 0.19	97.27 ± 0.27
R^2	0.982	0.830	0.895
x^2	0.00213	0.113	0.00684

It was also found that the values of q_e, k_1, k_2 and A increased while value of B decreased with when temperature increased for both Cu^{2+} and MB adsorption.

The adsorbate transport from the solution phase to the surface of the adsorbent particles occurs in several steps. The overall adsorption process may be controlled either by one or more steps, e.g., film or external diffusion, pore diffusion, surface diffusion and adsorption on the pore surface, or a combination of more than one step. The possibility of intra-particle diffusion was explored by using the intra-particle diffusion model (Cheung et al., 2000):

$$q_t = K_{id} t^{1/2} + C_i \quad (5)$$

where K_{id} is the intra-particle diffusion rate constant (g mg^{-1} min$^{-1/2}$), C is the constant (mg g^{-1}) that gives idea about the thickness of the boundary layer, i.e., larger the value of C the greater is the boundary layer effect.

Fig. 5 presented the plots of q_t versus $t^{1/2}$ for Cu^{2+} and MB adsorption. In Fig. 5, the data points were related by two straight lines for Cu^{2+} and three lines for MB, respectively. The first straight portion depicted macro-pore diffusion and the second represented micro-pore diffusion (Srivastava, Swamy, Mall, Prasad, & Mishra, 2006).

If the plot of q_t versus $t^{1/2}$ gives a straight line, then the sorption process is controlled by intra-particle diffusion only. However, if the data exhibit multi-linear plots, then two or more steps influence the sorption process. It is assumed that the external resistance to mass transfer surrounding the particles is significant only in the early stages of adsorption. This is represented by first sharper portion. The second or third linear portion is the gradual adsorption stage with intra-particle diffusion dominating (Srivastava et al., 2006).

The values of K_{id} and C_i were also listed in Tables 1 and 2. From Tables 1 and 2, the constants of C_i were not zero, the lines did not pass through the origin. This showed that pore diffusion was not the rate limiting step. So the adsorption process may be of a complex nature consisting of both surface adsorption and intra-particle diffusion (Vadivelan & Kumar, 2005). Furthermore, all these suggest that the adsorption of Cu^{2+} and MB over MWS may be controlled by external mass transfer followed by intra-particle diffusion mass transfer.

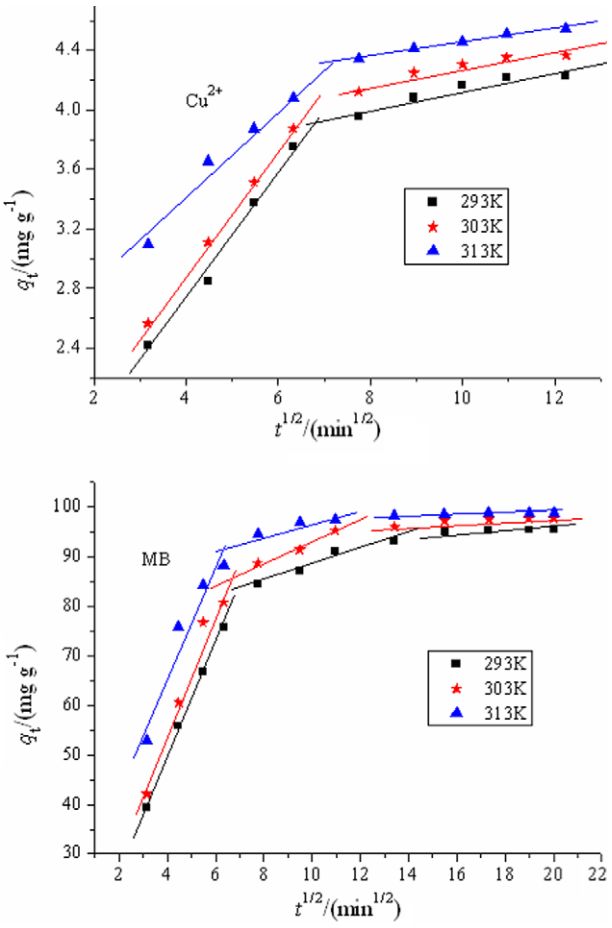

Fig. 5. Intra-particle diffusion plots for Cu^{2+} and MB adsorption of onto MWS.

Obviously, K_{i1} is larger than K_{i2} from Table 1 while C_1 was smaller than C_2. The value of R^2 in first adsorption step is also larger than that in second step. This shows that the intra-particle diffusion can predict the kinetic process at different stage.

3.3. Adsorption equilibrium study

For equilibrium study, the contact time is 4 h for Cu^{2+} and 8 h for MB in order to obtain the state of equilibrium, respectively. The effect of initial concentration of Cu^{2+} and MB on adsorption was shown in Fig. 6, respectively. The values of q_e increased with increasing c_0. The initial concentration provided the necessary driving force to overcome the resistances to the mass transfer of adsorbents between the aqueous and solid phases. The increase in c_0 also enhanced the interaction between adsorbents and MWS. Therefore, an increase in c_0 enhanced the adsorption uptake of metal and dye ions. The bigger adsorptive capacity was also observed in the higher temperature range. But the change was not significant.

Using linear regressive method, the correlation of q_e and c_0 at different temperature was listed in Table 3. R^2 was determined coefficient of the regressive analysis.

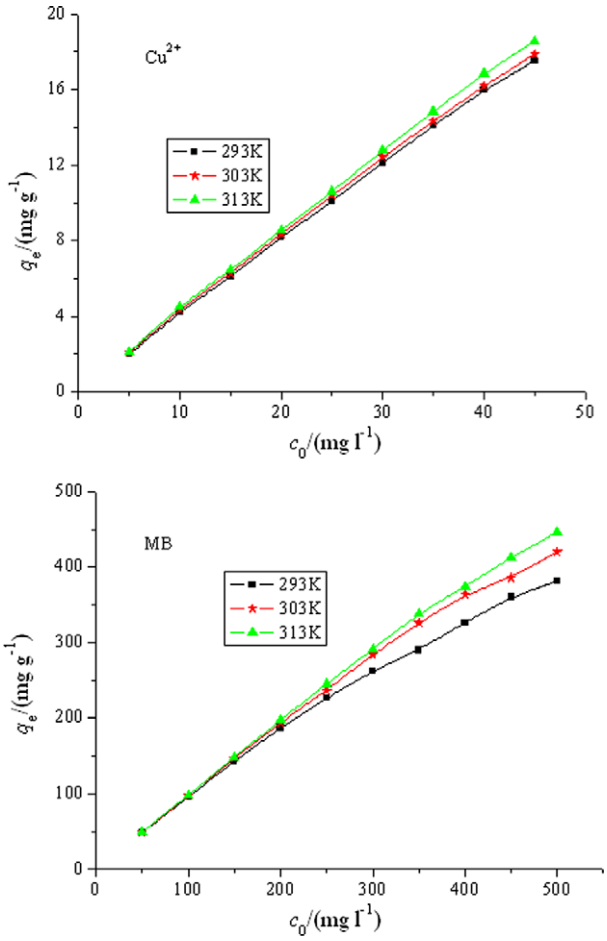

Fig. 6. Equilibrium quantities of Cu^{2+} and MB at different initial concentrations with different temperature.

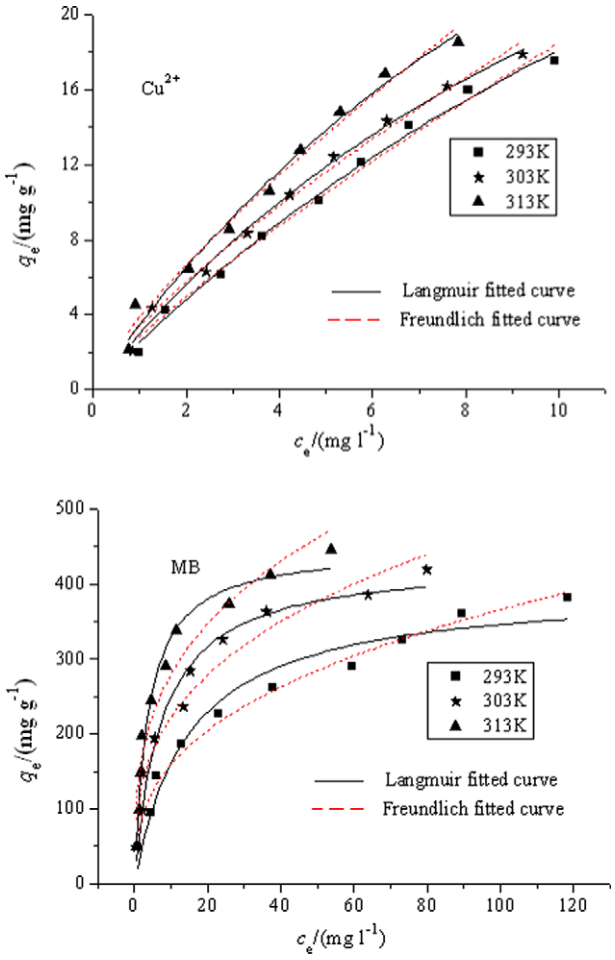

Fig. 7. The isotherms of Cu^{2+} and MB adsorption on MWS at three temperatures.

From 293 K to 313 K, the slope of the regressive line became larger, but the range was small. Furthermore, the quantity of Cu^{2+} or MB onto MWS was linear to the initial concentration within the range of experimental concentration with higher R^2 at three temperatures. Moreover, the values of R^2 for Cu^{2+} were bigger than for MB.

Analysis of the equilibrium data is important to develop an equation which accurately represents the results and which could be used for design purposes. The adsorption isotherms were presented in Fig. 7. The trend of quantity with c_e change was similar to that with c_0 change.

Two adsorption isotherms of Langmuir and Freundlich were employed to fit equilibrium data. The Langmuir adsorption isotherm has been successfully applied to many pollutants adsorption processes and has been the most widely used sorption isotherm for the sorption of a solute from a liquid solution (Langmuir, 1916). The commonly form of the Langmuir isotherm is:

$$q_e = \frac{q_m K_L c_e}{1 + K_L c_e} \quad (6)$$

Table 3
The relation between the amount of Cu^{2+} and MB adsorbed onto per unit mass of MWS (q_e) and the initial concentration (c_0).

T/K	Adsorption equation Cu^{2+}	R^2	Adsorption equation MB	R^2
293	$q_e = 0.3993c_0$	0.998	$q_e = 0.8227c_0$	0.975
303	$q_e = 0.4074c_0$	0.998	$q_e = 0.8948c_0$	0.985
313	$q_e = 0.4215c_0$	0.999	$q_e = 0.94351c_0$	0.993

where q_m is the q_e for a complete monolayer (mg g^{-1}), a constant related to adsorption capacity; and K_L is a constant related to the affinity of the binding sites and energy of adsorption (l mg^{-1}).

Freundlich isotherm is an empirical equation describing adsorption onto a heterogeneous surface. The Freundlich isotherm is commonly presented as (Freundlich, 1906):

$$q_e = K_F c^{1/n} \quad (7)$$

where K_F and $1/n$ are the Freundlich constants related to the adsorption capacity and adsorption intensity of the adsorbent, respectively.

The parameters of the two isotherms based on Eqs. (6) and (7) were presented in Table 4 using nonlinear regressive analysis.

From Table 4, the values of q_m, K_L and K_F increased with temperature rise for Cu^{2+} and MB adsorption, respectively. The obtained values of $1/n$ ($0.1 < 1/n < 1$) indicated a higher adsorb ability of MB at all temperatures studied (Raji & Anirudhan, 1998). From values of R^2 and x^2, both isotherm models can be used to predict the equilibrium behavior. The comparison of experimental points and fitted curves in Fig. 7 reinforced this result.

From the experimental result, the quantity of Cu^{2+} adsorption at equilibrium concentration 9.92 mg l^{-1} was 17.55 mg g^{-1}, while for MB adsorption it was 381.5 g mg g^{-1} at the concentration 118.5 mg l^{-1}. The maximal equilibrium quantity of Cu^{2+} and MB from Langmuir model on MWS was 39.17 and 396.9 mg g^{-1} at 293 K, respectively. For comparison of adsorption quantity of different materials, Table 5 listed values of q_m about some plant-derived absorbents, commercial activated carbon (AC) and ion exchange resin for adsorption quantity of Cu^{2+} and MB, respec-

Table 4
Isotherm constants for Cu^{2+} and MB adsorption onto MWS at different temperatures.

T/K	293	303	313
Langmuir Cu^{2+}			
K_L/(l mg^{-1})	0.0442 ± 0.0094	0.0655 ± 0.0101	0.0665 ± 0.0198
q_m/(mg g^{-1})	39.17 ± 9.60	48.25 ± 5.23	55.42 ± 12.15
R^2	0.994	0.995	0.986
x^2	0.190	0.156	0.507
Freundlich Cu^{2+}			
K_F	2.80 ± 0.22	3.37 ± 0.23	3.85 ± 0.32
$1/n$	0.819 ± 0.041	0.769 ± 0.036	0.784 ± 0.049
R^2	0.990	0.991	0.985
x^2	0.325	0.302	0.549
Langmuir MB			
K_L/(l mg^{-1})	0.0685 ± 0.0137	0.136 ± 0.024	0.272 ± 0.032
q_m/(mg g^{-1})	396.9 ± 21.5	432.8 ± 20.7	450.0 ± 14.4
R^2	0.961	0.967	0.982
x^2	555.2	593.2	362.1
Freundlich MB			
K_F	69.14 ± 5.63	104.2 ± 11.8	136.2 ± 14.5
$1/n$	0.362 ± 0.020	0.329 ± 0.031	0.312 ± 0.034
R^2	0.987	0.955	0.936
x^2	190.4	804.5	1310.8

tively. From Table 5, it was observed that the values of q_m about MWS for Cu^{2+} and MB were higher than natural wheat straw, other agricultural by-products and commercial AC. So the adsorption capacity of wheat straw was improved by chemical modification. It was also seen that the capacity of MWS for Cu^{2+} adsorption was smaller than that of ion exchange resin, but for MB adsorption it was nearly equal or lower. The adsorption capacity differences of metal and dye uptake are due to the properties of each adsorbent such as structure, functional groups and surface area and the experimental condition. From values of Table 5, MWS can be used to remove Cu^{2+} and MB from solution.

3.4. Thermodynamic parameters

3.4.1. Calculation of the change free energy change (ΔG^0)

To estimate the effect of temperature on the adsorption of MB onto zeolite, the free energy change (ΔG^0), enthalpy change (ΔH^0), and entropy change (ΔS^0) were determined. The adsorption process can be summarized which represents a heterogeneous equilibrium. The apparent equilibrium constant (K'_c) of the biosorption is defined as (Aksu, 2002):

$$K'_c = c_{ad,e}/c_e \tag{8}$$

where $c_{ad,e}$ is the concentration of adsorbate on the adsorbent at equilibrium (mg l^{-1}). The value of K'_c in the lowest experimental adsorbate concentration can be obtained. The K'_c value is used in the following equation to determine the change of Gibbs free energy of adsorption (ΔG^0).

$$\Delta G^0 = -RT \ln K'_c \tag{9}$$

The change of enthalpy (ΔH^0) and entropy (ΔS^0) can be obtained from the slope and intercept of a van't Hoff equation of ΔG^0 versus T.

$$\Delta G^0 = \Delta H^0 - T\Delta S^0 \tag{10}$$

where ΔG^0 is standard Gibbs free energy change, J; R is universal gas constant, 8.314 J mol^{-1} K^{-1} and T is absolute temperature, K.

Values of the standard Gibbs free energy change for the adsorption process obtained from Eq. (9) were listed in Table 6.

The negative values of ΔG^0 at all temperatures indicate the spontaneous nature of the adsorption of Cu^{2+} and MB on MWS. The negative value of ΔG^0 decreased with an increase in temperature, indicating that a better adsorption is actually obtained at higher temperatures. Moreover, the value of ΔG^0 for multilayer adsorption is more than −20 kJ mol^{-1} and less than zero. It should be noted that the magnitude of ΔG^0 values was in the range of multilayer adsorption (Bekci, Seki, & Yurdakoc, 2006).

The standard enthalpy and entropy changes of adsorption determined from the Eq. (10) were 12.68 kJ mol^{-1} and 54.8 J mol^{-1} K^{-1} for Cu^{2+}, 21.92 kJ mol^{-1} and 108 J mol^{-1} K^{-1} for MB, respectively. The positive value of ΔH^0 suggests the endothermic nature of adsorption. The positive value of ΔS^0 confirmed the increased randomness at the solid-solute interface during adsorption process, which suggests that Cu^{2+} and MB ions replace some water molecules from the solution previously adsorbed on the surface of adsorbent. These displaced molecules gain more translation

Table 5
Cu^{2+} and MB adsorption by different materials: q_m obtained from the Langmuir constant.

q_m/(mg g^{-1})	Adsorbent	References
Cu^{2+}		
4.46	Cereal chaff	Han, Zhang, et al. (2006)
8.3	Wheat shell	Basci, Kocadagistan, and Kocadagistan (2004)
5.40	Soybean straw	Šæiban et al. (2008)
1.85	Rice shell	Aydin, Bulut, and Yerlikaya (2008)
20.97	Sugar beet pulp	Reddad et al. (2002)
5.08	Commercial AC	Hawari (2004)
3.60	Commercial AC	Periasamy and Namasivayam (1996)
180	Ion exchange resin	Raghavan and Bhatt (1998)
100	Ion exchange resin	Raghavan and Bhatt (1998)
61.64	Ion exchange resin	Hawari (2004)
127.1	Ion exchange resin	Hawari (2004)
7.05	Wheat straw	Wu et al. (2009)
39.17	MWS	This study
MB		
40.6	Rice husk	Vadivelan and Kumar (2005)
20.3	Cereal chaff	Han, Wang, et al. (2006)
80.9	Phoenix tree leaves	Han et al. (2007)
16.56	Wheat shell	Bulut and Aydın (2006)
200	Commercial AC	Bestani, Benderdouche, Benstaali, Belhakem, and Addou (2008)
306	Ion exchange resin	Gut, Schiek, Haefeli, Walter-Sack, and Burhenne (2008)
384	Ion exchange resin	Gut et al. (2008)
1500–2100	Ion exchange resin	Gut et al. (2008)
60.66	Wheat straw	Wu et al. (2009)
396.9	MWS	This study

Table 6
Thermodynamic parameters of Cu^{2+} and MB adsorption on MWS.

Adsorbate	Cu^{2+}			MB		
T/K	293	303	313	293	303	313
ΔG^0/(kJ mol^{-1})	−3.36	−3.98	−4.46	−9.96	−11.22	−12.14
ΔH^0/(kJ mol^{-1})		12.68			21.92	
ΔS^0/(kJ mol^{-1} K^{-1})		0.0548			0.108	
E_a/(kJ mol^{-1})		20.91			24.24	

entropy than is lost by the adsorbate ions, thus allowing the prevalence of randomness in the system (Malkoc & Nuhoglu, 2007). The low value of ΔS^0 also indicated that no remarkable changed on entropy occurs.

3.4.2. Estimation of activation energy

The magnitude of activation energy may give an idea about the type of sorption. There are two main types of adsorption: physical and chemical. Activated chemical adsorption means that the rate varies with temperature according to a finite activation energy (8.4–83.7 kJ mol^{-1}) in the Arrhenius equation. In nonactivated chemical adsorption, the activation energy is near zero (Aksu, 2002).

The activation energy for MB adsorption was calculated by the Arrhenius equation:

$$k = k_0 e^{-\frac{E_a}{RT}} \quad (11)$$

where k_0 is the temperature independent factor in g mg^{-1} min^{-1}, E_a is the apparent activation energy of the reaction of adsorption in kJ mol^{-1}, R is the gas constant, 8.314 J mol^{-1} K^{-1} and T is the adsorption absolute temperature, K. The linear form is:

$$\ln k = -\frac{E_a}{RT} + \ln k_0 \quad (12)$$

When $\ln k$ is plotted versus $1/T$, a straight line with slope $-E_a/R$ is obtained.

The values of rate constant obtained nonlinear analysis according to the pseudo-second-order can be used to calculate the activation energy of sorption process. The energy of activation (E_a) was determined from the slope of the Arrhenius plot of $\ln k_2$ versus $1/T$ (figure not shown) according to Eq. (12) and was found to be 20.91 and 24.24 kJ mol^{-1} for Cu^{2+} and MB, respectively. The values are of the same magnitude as the activation energy of activated chemical sorption. The positive values of E_a suggested that rise in temperature favor the adsorption and adsorption process may be an endothermic in nature.

3.4.3. Estimation of diffusion coefficient

The half-adsorption time $t_{1/2}$ is another parameter which can be calculated from the equilibrium concentration and the diffusion coefficient rate values. This was calculated by using the following equation (Dogan, Ozdemir, & Alkan, 2007):

$$t_{1/2} = \frac{1}{k_2 q_e} \quad (13)$$

where k_2 and q_e can be obtained from Tables 2 and 3.

The diffusion coefficient for the intra-particle transport of the adsorbates was also calculated by using the following relationship (Dogan et al., 2007):

$$t_{1/2} = \frac{0.03r^2}{D} \quad (14)$$

where $t_{1/2}$ is the half life in seconds as calculated from Eq. (13), r is the radius of the adsorbent particle in centimeters and D is the diffusion coefficient value in cm^2 s^{-1} For the calculation of r value, it is assumed that the solid phase consists of particles which are spherical in nature. Calculated values of $t_{1/2}$ and D at 293 K were 9.97 min and 1.19×10^{-5} cm^2 s^{-1} for Cu^{2+} and 14.81 min and 8.04×10^{-6} cm^2 s^{-1} for MB, respectively.

The values of pore diffusion rate constants were found to be on the order of 10^{-10}–10^{-11} cm^2 s^{-1} for all the adsorbent samples, so the pore diffusion in this study was not significant (Dogan et al., 2007).

4. Conclusion

This study showed the characterization of MWS and Cu^{2+} and MB adsorption behavior by MWS. The NWS and MWS was mainly composed of cellulose, lignin and there were more carbonyl group on the surface of MWS. The equilibrium adsorption can be fitted by Langmuir and Freundlich model for Cu^{2+} and MB adsorption. The kinetic process can be predicted by pseudo-second-order model. The adsorption may be controlled by external mass transfer followed by intra-particle diffusion mass transfer. The thermodynamics parameters indicated spontaneous and endothermic process. Rise in temperature favored the adsorption. As the higher adsorption quantity of MWS, it may be concluded that MWS may be used for elimination of metal and dye ions from wastewater.

Acknowledgments

This work was supported by the National Natural Science Foundation of China (J0830412), the China Postdoctoral Science Foundation (20070420811) and the Natural Science Foundation of Henan Province.

References

Ahluwalia, S. S., & Goyal, D. (2007). Microbial and plant derived biomass for removal of heavy metals from wastewater. *Bioresource Technology, 98*, 2243–2257.
Aksu, Z. (2002). Determination of the equilibrium, kinetic and thermodynamic parameters of the batch biosorption of nickel(II) ions onto *Chlorella vulgaris*. *Process Biochemistry, 38*, 89–99.
Aksu, Z., & Isoglu, I. A. (2007). Use of dried sugar beet pulp for binary biosorption of Gemazol Turquoise Blue-G reactive dye and copper(II) ions: Equilibrium modeling. *Chemical Engineering Journal, 127*, 177–188.
Aydın, H., Bulut, Y., & Yerlikaya, C. (2008). Removal of copper (II) from aqueous solution by adsorption onto low-cost adsorbents. *Journal of Environmental Management, 87*, 37–45.
Basci, N., Kocadagistan, E., & Kocadagistan, B. (2004). Biosorption of copper(II) from aqueous solutions by wheat shell. *Desalination, 164*, 135–140.
Bekci, Z., Seki, Y., & Yurdakoc, M. K. (2006). Equilibrium studies for trimethoprim adsorption on montmorillonite KSF. *Journal Hazardous Materials, 133*, 233–242.
Bestani, B., Benderdouche, N., Benstaali, B., Belhakem, M., & Addou, A. (2008). Methylene blue and iodine adsorption onto activated desert plant. *Bioresource Technology, 17*, 8441–8444.
Bulut, Y., & Aydın, H. (2006). A kinetics and thermodynamics study of methylene blue adsorption on wheat shells. *Desalination, 194*, 259–267.
Cheung, C. W., Porter, J. F., & Mckay, G. (2000). Sorption kinetics for the removal of copper and zinc from effluents using bone char. *Separation and Purification Technology, 19*, 55–64.
Cimino, G., Passerini, A., & Toscano, G. (2000). Removal of toxic cations and Cr (VI) from aqueous solution by hazelnut shell. *Water Research, 34*, 2955–2962.
Crini, G. (2006). Non-conventional low-cost adsorbents for dye removal: A review. *Bioresource Technology, 97*, 1061–1085.
Dang, V. B. H., Doan, H. D., Dang-Vuc, T., & Lohi, A. (2009). Equilibrium and kinetics of biosorption of cadmium(II) and copper(II) ions by wheat straw. *Bioresource Technology, 100*, 211–219.
Doan, H. D., Lohi, A., Dang, V. B. H., & Dang-Vu, T. (2008). Removal of Zn^{+2} and Ni^{+2} by adsorption in a fixed bed of wheat straw. *Process Safety and Environmental Protection, 86*, 259–267.
Dogan, M., Ozdemir, Y., & Alkan, M. (2007). Adsorption kinetics and mechanism of cationic methyl violet methylene blue dyes onto sepiolite. *Dyes and Pigments, 75*, 701–713.
Freundlich, H. M. F. (1906). Uber die adsorption in lasungen. *Journal of Physical Chemistry, 57*, 385–470.
Gong, R. M., Sun, J., Zhang, D. M., Zhong, K. D., & Zhu, G. P. (2008). Kinetics and thermodynamics of basic dye sorption on phosphoric acid esterifying soybean hull with solid phase preparation technique. *Bioresource Technology, 99*, 4510–4514.

Gong, R. M., Zhong, K. D., Hu, Y., Chen, J., & Zhu, G. P. (2008). Thermochemical esterifying citric acid onto lignocellulose for enhancing methylene blue sorption capacity of rice straw. *Journal of Environmental Management, 88*, 875–880.

Gong, R. M., Zhu, S. X., Zhang, D. M., Chen, J., Ni, S. J., & Guan, R. (2008). Adsorption behavior of cationic dyes on citric acid esterifying wheat straw: Kinetic and thermodynamic profile. *Desalination, 230*, 220–228.

Gupta, V. K., & Ali, I. (2008). Removal of endosulfan and methoxychlor from water on carbon slurry. *Environmental and Science Technology, 42*, 766–770.

Gupta, V. K., Jain, R., & Varshney, S. (2007). Removal of Reactofix golden yellow 3 RFN from aqueous solution using wheat husk – An agricultural waste. *Journal Hazardous Materials, 142*, 443–448.

Gupta, V. K., Mittal, A., Krishnan, L., & Mittal, J. (2006). Adsorption treatment and recovery of the hazardous dye, Brilliant Blue FCF, over bottom ash and de-oiled soya. *Journal of Colloid and Interface Science, 293*, 16–26.

Gupta, V. K., & Suhas, M. (2009). Application of low-cost adsorbents for dye removal – A review. *Journal of Environmental Management, 90*, 2313–2342.

Gurgel, L. V. A., Freitas, R. P., & Gil, L. F. (2008). Adsorption of Cu(II), Cd(II), and Pb(II) from aqueous single metal solutions by sugarcane bagasse and mercerized sugarcane bagasse chemically modified with succinic anhydride. *Carbohydrate Polymers, 74*, 922–929.

Gut, F., Schiek, W., Haefeli, W. E., Walter-Sack, I., & Burhenne, J. (2008). Cation exchange resins as pharmaceutical carriers for methylene blue: Binding and release. *European Journal of Pharmaceutics and Biopharmaceutics, 69*, 582–587.

Han, R. P., Ding, D. D., Xu, Y. F., Zou, W. H., Wang, Y. F., Li, Y. F., et al. (2008). Use of rice husk for the adsorption of congo red from aqueous solution in column mode. *Bioresource Technology, 99*, 2938–2946.

Han, R. P., Han, P., Cai, Z. H., Zhao, Z. H., & Tang, M. S. (2008). Kinetics and isotherms of neutral red adsorption on peanut husk. *Journal of Environmental Science, 20*, 1035–1041.

Han, R. P., Wang, Y. F., Han, P., Shi, J., Yang, J., & Lu, Y. S. (2006). Removal of methylene blue from aqueous solution by chaff in batch mode. *Journal Hazardous Materials, 137*, 550–557.

Han, R. P., Wang, Y., Zhao, X., Wang, Y. F., Xie, F. L., Cheng, J. M., et al. (2009). Adsorption of methylene blue by phoenix tree's leaf powder in fixed-bed column: Experiments and prediction of breakthrough curves. *Desalination, 245*, 284–297.

Han, R. P., Zhang, J. J., Han, P., Wang, Y. F., Zhao, Z. H., & Tang, M. S. (2009). Study of equilibrium, kinetic and thermodynamic parameters about methylene blue adsorption onto natural zeolite. *Chemical Engineering Journal, 145*, 496–504.

Han, R. P., Zhang, J. H., Zhu, L., Zou, W. H., & Shi, J. (2006). Determination of the equilibrium, kinetic and thermodynamic parameters of the batch biosorption of copper(II) ions onto Chaff. *Life Science Journal, 3*, 81–88.

Han, R. P., Zhang, J. H., Zou, W. H., Shi, J., & Liu, H. M. (2005). Equilibrium biosorption isotherm for lead ion on chaff. *Journal Hazardous Materials, 125*, 266–271.

Han, R. P., Zou, W. H., Yu, W. H., Cheng, S. J., Wang, Y. F., & Shi, J. (2007). Biosorption of methylene blue from aqueous solution by fallen phoenix tree's leaves. *Journal Hazardous Materials, 141*, 156–162.

Hawari, A. A. (2004). Biosorption of lead, copper, cadmium and nickel by anaerobic biomass. Ph.D. Dissertation, Concordia University, Canada.

Ho, Y. S., & McKay, G. (1999). Pseudo-second-order model for sorption process. *Process Biochemistry, 34*, 451–465.

Ho, Y. S., Ng, J. C. Y., & McKay, G. (2000). Kinetics of pollutant sorption by biosorbents: Review. *Separation and Purification Methods, 29*, 189–232.

Khan, E., Li, M., & Huang, C. P. (2008). Hazardous waste treatment technologies. *Water Environmental Research, 80*, 1654–1708.

Krishnani, K. K., Meng, X. G., Christodoulatos, C., & Boddu, V. M. (2008). Biosorption mechanism of nine different heavy metals onto biomatrix from rice husk. *Journal Hazardous Materials, 153*, 1222–1234.

Langmuir, I. (1916). The constitution and fundamental properties of solids and liquids. *Journal of America Chemical Society, 38*, 2221–2295.

Malkoc, E., & Nuhoglu, Y. (2007). Determination of kinetic and equilibrium parameters of the batch adsorption of Cr(VI) onto waste acorn of *Quercus ithaburensis*. *Chemical Engineering Process, 46*, 1020–1029.

Marshall, W. E., Wartelle, L. H., Boler, D. E., Johns, M. M., & Toles, C. A. (1999). Enhanced metal adsorption by soybean hulls modified with citric acid. *Bioresource Technology, 69*, 263–268.

O'Connell, D. W., Birkinshaw, C., & O'Dwyer, T. F. (2008). Heavy metal adsorbents prepared from the modification of cellulose: A review. *Bioresource Technology, 99*, 6709–6724.

Ong, S. T., Lee, C. K., & Zainal, Z. (2007). Removal of basic and reactive dyes using ethylenediamine modified rice hull. *Bioresource Technology, 98*, 2792–2799.

Periasamy, K., & Namasivayam, C. (1996). Removal of copper(II) by adsorption onto peanut hull carbon from water and copper plating industry wastewater. *Chemosphere, 32*, 769–789.

Raghavan, R., & Bhatt, C. V. (1998). Comparative study of certain ion-exchange resins for application in copper-bearing process solutions. *Hydrometallurgy, 50*, 169–183.

Raji, C., & Anirudhan, T. S. (1998). Batch Cr(VI) removal by polyacrylamide-grafted sawdust: Kinetics and thermodynamics. *Water Research, 32*, 3772–3780.

Reddad, Z., Gerente, C., Andres, Y., Ralet, M. C., Thibault, J. F., & Cloirec, P. L. (2002). Ni (II) and Cu (II) binding properties of native and modified sugar beet pulp. *Carbohydrate Polymer, 49*, 23–31.

Robinson, T., Chandran, B., & Nigam, P. (2002). Removal of dyes from a synthetic textile dye effluent by biosorption on apple pomace and wheat straw. *Water Research, 36*, 2824–2830.

Šæiban, M., Klašnja, M., & Škrbiæ, B. (2008). Adsorption of copper ions from water by modified agricultural by-products. *Desalination, 229*, 170–180.

Srivastava, V. C., Swamy, M. M., Mall, I. D., Prasad, B., & Mishra, I. M. (2006). Adsorptive removal of phenol by bagasse fly ash and activated carbon: Equilibrium, kinetics and thermodynamics. *Colloids Surfaces A: Physicochemical and Engineering Aspects, 272*, 89–104.

Sud, D., Mahajan, G., & Kaur, M. P. (2008). Agricultural waste material as potential adsorbent for sequestering heavy metal ions from aqueous solutions – A review. *Bioresource Technology, 99*, 6017–6027.

Teixeira Tarley, C. R., & Zezzi Arruda, M. A. (2004). Biosorption of heavy metals using rice milling by-products. Characterisation and application for removal of metals from aqueous effluents. *Chemosphere, 54*, 987–995.

Tsang, Daniel C. W., Hu, J., Liu, Mei Y., Zhang, W. H., Lai, Keith C. K., & Lo, Irene M. C. (2007). Activated carbon produced from waste wood pallets: Adsorption of three classes of dyes. *Water, Air & Soil Pollution, 184*, 141–155.

Vadivelan, V., & Kumar, K. V. (2005). Equilibrium, kinetics, mechanism, and process design for the sorption of methylene blue onto rice husk. *Journal of Colloid and Interface Science, 286*, 90–100.

Vaughan, T., Seo, C. W., & Marshall, W. E. (2001). Removal of selected metal ions from aqueous solution using modified corncobs. *Bioresource Technology, 78*, 133–139.

Wan Ngah, W. S., & Hanafiah, M. A. K. M. (2008). Removal of heavy metal ions from wastewater by chemically modified plant wastes as adsorbents: A review. *Bioresource Technology, 99*, 3935–3948.

Wang, S. B., & Ariyanto, E. (2007). Competitive adsorption of malachite green and Pb ions on natural zeolite. *Journal of Colloid and Interface Science, 314*, 25–31.

Wong, K. K., Lee, C. K., Low, K. S., & Haron, M. J. (2003). Removal of Cu and Pb by tartaric acid modified rice husk from aqueous solutions. *Chemosphere, 50*, 23–28.

Wu, Y. J., Zhang, L. J., Gao, C. L., Ma, J. Y., Ma, X. H., & Han, R. P. (2009). Adsorption of copper ions and methylene blue in single and binary system on wheat straw. *Journal of Chemical and Engineering Data*. doi:10.1021/je900220q.